Microbial Ecology (2020) 80:47–59
https://doi.org/10.1007/s00248-019-01470-z

ENVIRONMENTAL MICROBIOLOGY

Emergence of a Synergistic Diversity as a Response to Competition in *Pseudomonas putida* Biofilms

Arnaud Bridier[1,2] · J. C. Piard[3] · R. Briandet[3] · T. Bouchez[2]

Received: 17 May 2019 / Accepted: 1 December 2019 / Published online: 16 December 2019

Abstract

Genetic diversification through the emergence of variants is one of the known mechanisms enabling the adaptation of bacterial communities. We focused in this work on the adaptation of the model strain *Pseudomonas putida* KT2440 in association with another *P. putida* strain (PCL1480) recently isolated from soil to investigate the potential role of bacterial interactions in the diversification process. On the basis of colony morphology, three variants of *P. putida* KT2440 were obtained from co-culture after 168 h of growth whereas no variant was identified from the axenic KT2440 biofilm. The variants exhibited distinct phenotypes and produced biofilms with specific architecture in comparison with the ancestor. The variants better competed with the *P. putida* PCL1480 strain in the dual-strain biofilms after 24 h of co-culture in comparison with the ancestor. Moreover, the synergistic interaction of KT2440 ancestor and the variants led to an improved biofilm production and to higher competitive ability versus the PCL1480 strain, highlighting the key role of diversification in the adaptation of *P. putida* KT2440 in the mixed community. Whole genome sequencing revealed mutations in polysaccharides biosynthesis protein, membrane transporter, or lipoprotein signal peptidase genes in variants.

Keywords Biofilm · *Pseudomonas putida* · Species interactions · Confocal microscopy · Synergistic populations · Adaptation · Genetic variants

Introduction

In natural and domesticated environments, bacteria are most of the time present as surface-associated communities known as biofilms [1]. The formation of such communities is governed by a complex network of environmental and intercellular cues, and bacterial interactions play a central role in the architectural development and functional properties of biofilms [2–4]. Natural microbial communities are indeed recognized as complex associations of many bacterial strains or species, and numerous studies highlighted the importance of bacterial cooperation in the performing of essential functions such as biofilm formation, methanogenesis, or pollutant degradation for instance [5–8]. In the medical area, it has been shown that, due to species interactions, multispecies communities can display higher resistance to antibiotics and disinfectants than those observed for each individual species separately in monoculture biofilms [9–11]. Since microbial biofilms are dynamic environments prone to constant evolution during their development and maturation, bacterial interactions also evolve over time, illustrating the adaptation of the bacterial community to both the environmental conditions and the bacterial community members [12–14]. Genetic diversification and production of variants with specific phenotypes is one of the known mechanisms enabling this adaptation [15]. This self-generated diversity could provide a form of biological insurance that can safeguard the community facing adverse conditions [16]. In the last years, various experimental models were developed and used to study diversification observed during biofilm evolution and the derived associated advantages and disadvantages [17, 18]. Such diversification has been shown in a wide variety of monocultured bacterial species including *Streptococcus pneumonia*, *Staphylococcus*

✉ Arnaud Bridier
arnaud.bridier@anses.fr

[1] ANSES, Fougères Laboratory, AB2R, 10B rue Claude Bourgelat, 35300 Fougères, France

[2] IRSTEA, UR PROSE, 1 rue Pierre-Gilles de Gennes, 92761 Antony Cedex, France

[3] Institut Micalis, INRA, AgroParisTech, Université Paris-Saclay, 78350 Jouy-en-Josas, France

aureus, *Escherichia coli*, *Burkholderia cenocepacia*, *Pseudomonas aeruginosa, Pseudomonas fluorescens*, or *Vibrio cholerae* [15, 19–26]. For instance, the emergence of the small colony variant in *P. aeruginosa, V. cholerae*, *or Salmonella enterica* communities has often been associated with an increase ability to form biofilm, a higher resistance to stress, and/or a higher virulence compared with the wild-type strains [27–29]. However, only few studies addressed bacterial diversification in mixed bacterial biofilms and only few observations highlighted the influence of biotic environment in strain adaptation in mixed communities [30, 31]. Further knowledge in the mutual adaptation of bacterial species in mixed communities is however crucial in order to understand the close relationship between the mechanisms of this adaptation and the emergence of specific biofilm functions. By studying the coexistence of *Acinetobacter* sp. and *Pseudomonas putida*, Hansen et al. [31] showed that simple mutations in the genome of *P. putida* triggered its adaptation to the presence of *Acinetobacter* sp. after 5 days of growth in mixed biofilm. Due to a mutation in a gene involved in lipopolysaccharide biosynthesis, *P. putida* exhibited a better ability to form biofilm compared with the ancestor in the defined experimental conditions that led to an increase in both the stability and the productivity of the derived mixed community. Interestingly, this illustrates how a species can rapidly adapt to another in mixed communities and the fact that the new interaction occurring between "adapted" strains may lead to the emergence of new functional properties of the whole community. In the case of competitive or cooperative interactions between some strains [32], the equilibrium between bacterial strains or species can evolve and thus be changed when diversity emerges. Overall, the ambition to predict the functioning of complex ecosystems and their behavior in response to environmental changes requires understanding how species will evolve together [30]. In this context, the present study focused on the adaptation of the model strain *Pseudomonas putida* KT2440 (GFP-tagged) in mixed biofilm with another *P. putida* strain (PCL1480, mCherry-tagged) initially isolated from plant roots [33]. The KT2440 variants were phenotypically characterized and their genomes were fully sequenced. The role of variants and their interactions in the adaptation of strain KT2440 were then discussed in the light of identified mutations.

Materials and Methods

Strains and Growth Media

The results presented here were obtained using two autofluorescent strains: *Pseudomonas putida* KT2440 GFP (green), gentamicin and chloramphenicol resistant [34]; and *Pseudomonas putida* PCL1480 mCherry (red) gentamicin resistant [35]. Bacterial stock cultures were kept at − 80 °C in Tryptic Soy Broth (TSB, BioMérieux, France) containing 20% (vol/vol) glycerol. Prior to each experiment, frozen cells were subcultured overnight in TSB at 30 °C under agitation (180 rpm) and the resulting suspension was diluted and spread on Tryptic Soy Agar plates (TSA, BioMérieux, France) before incubation for 24 h at 30 °C. A colony was then transferred in M9 minimal medium (Sigma-Aldrich, USA) supplemented with glucose at 1 mg ml^{-1} (Sigma, France) and gentamicin at 10 μg ml^{-1} and then incubated under agitation (180 rpm) at 30 °C for 24 h.

Flow Cell Biofilm Experiments and Detection of Genetic Variants

Biofilms were grown in three channel flow cell systems (individual channel dimension of 1 × 4 × 40 mm) in M9 minimal medium supplemented with glucose at 1 mg ml^{-1} and gentamicin at 10 μg ml^{-1}. The flow systems were assembled and prepared as described previously by Weiss Nielsen et al. [36]. Flow cells were inoculated with a sterile syringe by injecting 1 ml of a 24-h bacterial suspension calibrated at OD_{600nm} = 0.01 (corresponding to ~ 10^6 CFU/ml). For dual-strain species biofilms, each bacterial suspension were adjusted to OD_{600nm} = 0.005 and mixed at a ratio of 1:1 in order to have the same number of cells adhered in the flow cell at the beginning of axenic and dual-strain biofilm experiments. Flow cells were left without flow for 1 h to allow bacteria to adhere to the glass substratum. Medium flow was then adjusted at 2 ml/h using a Watson Marlow 205S peristaltic pump and the system was incubated at 30 °C to allow biofilm development for different times (24 h, 72 h, 120 h, and 168 h) until confocal laser scanning microscopy (CLSM) observations.

For each observation after those time intervals, biofilm cells were harvested after CLSM observations from flow cell by aspirating and expelling 150 mM NaCl with sterile syringe in the adequate flow cell channel, and the cell suspension recovered was 10-fold serially diluted before being plated on TSA supplemented with chloramphenicol at 5 μg ml^{-1} and incubated at 30 °C for at least 48 h. The use of TSA plates supplemented by chloramphenicol enabled the selection of *P. putida* KT2440 GFP cells and derived variants (and the exclusion of *P. putida* PCL1480 mCherry and derivatives). Approximately 2000 colonies were examined at each time interval. Genetic stability of the variants was confirmed by assessing morphotype heritability after continued isolated passage on plates. The presence of variants was similarly investigated in a same manner from a planktonic suspension under agitation at 180 rpm associating *P. putida* KT2440 GFP and *P. putida* PCL1480 mCherry after 168 h of co-culture.

Confocal Laser Scanning Microscopy Observations and Image Analysis

Biofilms in flow cells were scanned using a Zeiss LSM 510 confocal microscope at the IRSTEA MIMOSE platform (Antony, France) using a × 40 oil objective lens with a 1.3 numerical aperture and a 488-nm argon laser set at 25% of its maximum intensity (GFP excitation) and/or a 543 nm-helium/neon laser at 50% of its maximum intensity (mCherry excitation). Emitted fluorescence was sequentially recorded within a range of 490 to 540 nm and within a range of 590 to 700 nm in order to capture GFP and mCherry fluorescence, respectively. A minimum of 10 z-stacks (z-step of 1 μm) was performed for each strain and each biofilm development time in at least two different channels. CLSM image stacks were processed using the COMSTAT program [37] to extract quantitative descriptors of biofilm structure such as biovolume. Biofilm 3D projections were reconstructed using the IMARIS software (Bitplane®, Switzerland) directly from confocal image stacks at the INRA MIMA2 imaging center (Massy, France).

Phenotypic Characterization of Genetic Variants

Cell Surface Characteristics

Cell surface hydrophobicity was determined by measuring the affinity of cells to hexadecane, an alkane hydrocarbon using the BATH method [38]. Briefly, bacterial cells were harvested from 24-h culture in M9 medium supplemented with glucose at 1 mg ml^{-1} by centrifugation (7000*g*, 10 min), washed twice, and suspended in 150 mM NaCl (absorbance at 400 nm adjusted to 0.8, precisely measured and noted A_i). Then, 2.4 ml of this bacterial suspension was mixed thoroughly for 60 s with 0.4 ml of hexadecane, and the mixture was left for 15 min at room temperature (20 °C) to ensure complete separation of the two phases before the measurement of absorbance at 400 nm of the aqueous phase (A_f). The percentage of cells in hexadecane layer was subsequently calculated using the equation: $100 \times (1\text{-}A_i/A_f)$. Each experiment was performed three times with two independent bacterial cultures.

Congo Red Indicator Assay on Macrocolonies

The morphology of macrocolonies formed by *P. putida* KT2440 GFP ancestor and variants and their Congo red-binding properties were tested using indicator agar plates. Experimentally, 5 μl of a 24-h culture in M9 minimal medium at 1 mg ml^{-1} of glucose was inoculated on TSA (1.5%) containing 40 μg/ml Congo Red (Sigma-Aldrich, France). Plates were then incubated for 72 h at 30 °C. Digital images of the macrocolonies on plates were taken using an Olympus C-5060 digital camera.

Pellicle Experiments

One hundred microliters of 24-h bacterial suspension was used to inoculate 10 ml of M9 medium at 1 mg ml^{-1} of glucose in sterile glass tubes. Tubes were then incubated at 30 °C, and pellicle formation was recorded at 72 h. Digital images of the pellicles in the tubes were taken using an Olympus C-5060 digital camera.

Swimming and Swarming Experiments

For swarming, 9-cm agar plates containing 20 ml of M9 medium at 1 mg ml^{-1} of glucose fortified with 0.8% agar were prepared and dried for 30 min with their lids open under a laminar flow hood. Ten microliters of 24-h bacterial suspension was then inoculated at the center of the swarming plates, dried for 15 min under the laminar flow hood, and incubated at 30 °C for 24 h. For swimming, 9-cm agar plates containing 20 ml of M9 medium at 1 mg ml^{-1} of glucose fortified with 0.3% agar were prepared and dried for 30 min with their lids open under a laminar flow hood. Five microliters of an overnight culture was then inoculated at the center of the plate, dried for 15 min, and incubated at 30 °C for 24 h. Digital images of the swarming and swimming plates were collected using an Olympus C-5060 digital camera.

Determination of Growth Rate of *P. putida* KT2440 Ancestor, Variants and Combination and Planktonic Competition Experiments with PCL1480 mCherry Strain

Growth parameters of *P. putida* KT2440 ancestor, variants, and combinations in M9 minimal medium supplemented with glucose as sole carbon source were obtained using an automatic Bioscreen C reader (Labsystem France SA, Les Ulis, France). This device generated turbidity growth curves of bacterial suspension in 100-well microtiter plates. Experimentally, M9 minimal medium solution containing 1 mg ml^{-1} of glucose was prepared and then, wells of the plates were each inoculated with 290 μl of the M9 medium solution. 10 microliters of 24-h bacterial suspension adjusted to $OD_{600nm} = 0.01$ was then added and the plates were incubated in the Bioscreen device which was set up to measure OD_{600nm} of *P. putida* suspensions every hour at 30 °C for 72 h with shaking before each measurement. Experiments were performed three times independently (three different microtiter plates) in triplicate (three wells per microtiter plate). The growth rates (μ) of the *P. putida* strains were extracted from the growth curves obtained using the modified Gompertz model as described by Cheroutre-Vialette et al. [39]. Planktonic competition tests were also performed to check if the mutations in variants also provide them an advantage in unstructured environment. In this aim, *P. putida* PCL1480 mCherry was mixed at a ratio of 1:1 with each of the variants

and WT in M9 minimal medium supplemented with glucose at 1 mg ml^{-1}, and the proportion of red and green cells were enumerated using CLSM after 24 h of co-culture.

Whole Genome Sequencing and Variation Analysis

DNA Extraction

A 2-ml aliquot of bacterial cultures in exponential growth phase was centrifuged at 10000*g* for 10 min, and total DNA was extracted from the pellet using the Powersoil™ DNA isolation kit (MoBio laboratories, Carlsbad, CA, USA) according to the manufacturer's instructions. The concentration of DNAs extracted was quantified using a quantifying fluorescent dye assay (Qubit dsDNA BR assay kits) and Qubit 2.0 Fluorometer (Invitrogen, Life Technologies, CA, USA).

Genome Sequencing

Whole genome sequencing was performed using the Ion Torrent PGM™ platform (life technologies) at IRSTEA MIMOSE platform (Antony, France). DNA libraries were prepared using 100 ng of total DNA using the Xpress™ Plus Fragment Library Kit. Enzymatic fragmentation of DNA was performed using the Ion Shear™ Plus Reagents. Xpress™ barcode adapters were used to identify each strain independently. Template preparation was achieved using the Ion OneTouch™ 400 v2 kit and Ion OneTouch™ 2 system. Sequencing was performed using a 316v2 chip and Ion PGM™ sequencing 400 kit. All the library, template, and sequencing preparations were carefully performed according to the manufacturer's instruction.

Sequences Analysis and Mutations Detection

The Ion Torrent suite software was used to carry out base calling and quality score calibration. Reads were trimmed and sorted according to their barcode before being aligned to the KT2440 reference genome. Aligned sequence was thereby exported for each variant in the BAM format. The probabilistic variant detection tool was then performed using this BAM files and the high-throughput sequencing module of CLC Genomics Workbench (version 6.0.1; CLC bio) to identify mutations present in variants compared with the reference KT2440 GFP sequence. Minimum coverage was set up at 15 and variant probability at 80%. Both the following additional filters were activated: "required presence in both forward and reverse read" and "filter 454/Ion homopolymer indels" in order to avoid false positive variants.

Statistical Analysis

Difference between biofilm biovolumes were assessed using one-way ANOVA with Microsoft Excel using the "Analysis Toolpak" add-in. Significance was defined as a *P* value associated with Fisher's test value lower than 0.05.

Results

Structural Dynamics of Single and Dual-Strain *P. putida* Biofilms

Biofilms formed by *P. putida* KT2440 GFP alone or in combination with *P. putida* PCL1480 mCherry were visualized using confocal laser scanning microscopy. Representative 3D reconstructions obtained for the different observation times and associated biovolumes were displayed in Fig. 1. Structural dynamics showed that *P. putida* KT2440 GFP was able to form large three-dimensional structures under our conditions and that biofilm biovolume reached maximum values after 120 h of development. When growing in dual-strain species biofilm, *P. putida* KT2440 GFP was outcompeted by the *P. putida* PCL1480 mCherry during the initial stages of biofilm formation. Indeed, biovolumes of the PCL1480 strain were significantly higher ($P < 0.05$) than those obtained for KT2440 GFP strain up to 120-h biofilm development (Fig. 1). However, dual-strain biofilm analysis at 168 h of development showed that both strains exhibited similar biovolumes mainly due to a decrease of the biovolume of the PCL1480 strain between 120 and 168 h of development.

Isolation and Phenotypic Characterization of *P. putida* KT2440 Variants

Biofilm cells were recovered from flow cell after the different observation time for mono- and bi-specific biofilms and spread on TSA plates (containing chloramphenicol to select KT2440 GFP strain and associated variants) after dilution. No variant of *P. putida* KT2440 GFP (referenced hereafter as WT) was detected in our conditions for mono-specific biofilms after all time of observations and neither after 24 h, 72 h, and 120 h in mixed biofilms with PCL1480 mCherry strain. We did not detect either any variant after a co-culture of 168 h in the same conditions in a planktonic suspension. In contrast, three variants were identified in the dual-strain biofilm detached after 168 h of development. The most abundant variant, constituting 5.6% of the total of ~ 2000 analyzed colonies, exhibited small colony compared with WT and was called "mini" (Fig. 2A). The second most abundant variant (1.6%) formed wrinkled colonies and was thus called "wrinkly" and the least abundant variant (0.6%) displayed rough colonies when compared with WT and was called "rough."

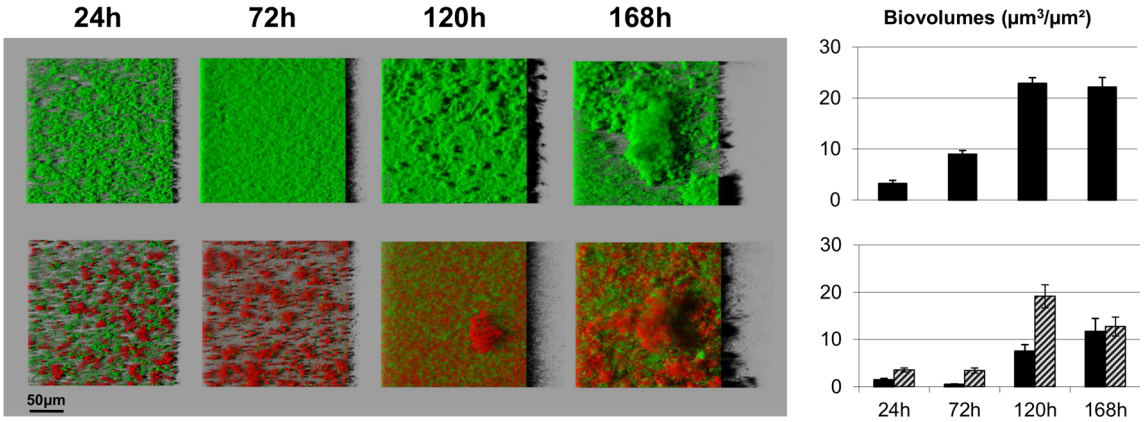

Fig. 1 Structural dynamics of *P. putida* KT2440 GFP (green) monospecies biofilm (upper panel) and mixed biofilm with the PCL180 mCherry strain (red) (lower panel) and associated biovolumes. Images correspond to the aerial view of biofilms with a virtual shadow projection on the right. In histograms, black bars correspond to the *P. putida* KT2440 GFP strain and dashed bars to the *P. putida* PCL1480 mCherry strain. Error bars represent the standard deviation obtained with 10 confocal image stacks

As displayed in Fig. 2, the three variants exhibited specific phenotypes compared with WT. The "mini" variant produced small cells in liquid cultures and its very high affinity to hexadecane (77.5 ± 2.5%) demonstrated a very high hydrophobicity of cell surface compared with WT (16.1 ± 4.8%). This variant also displayed an altered mobility in swimming plates because it did not colonize the plate except a small area close to the inoculation spot (Fig. 2D), whereas the WT invaded almost the whole plate. The cells of the "rough" variant formed chains and also exhibited an increased hydrophobicity compared with WT with a percentage of affinity to hexadecane equal to 65.5 ± 3.1%. The "wrinkly" variant also produced small cells in liquid cultures when compared with WT. On Congo red indicator plates, it produced large wrinkled macrocolonies which stained red more intensively (Fig. 2C). In addition, and contrary to the WT, it demonstrated the ability to swarm on semi-solid nutritive agar and to form pellicle at the air-medium interface in glass tubes (Fig. 2E, F). The

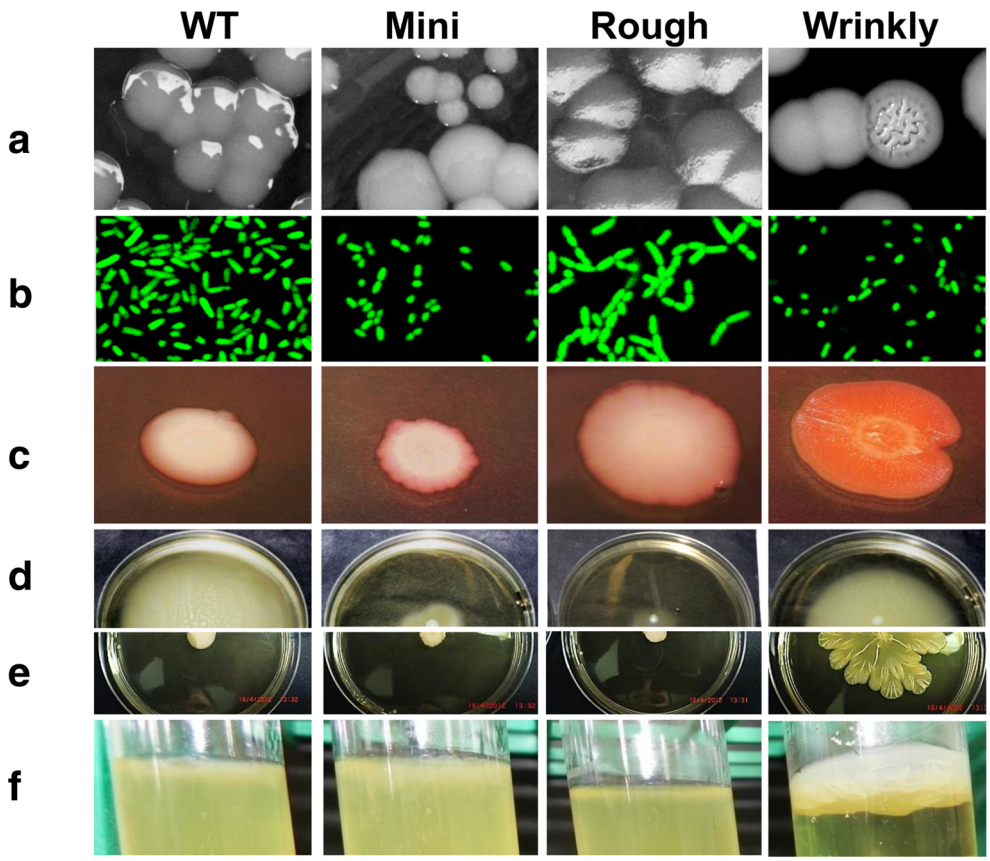

Fig. 2 Phenotypic characterization of variants. (A) Colony morphology on TSA petri dishes. (B) Cellular morphology. (C) Macrocolony structure on agar plates. (D) Swimming and (E) swarming abilities. (F) Pellicles formation in medium tubes

"wrinkly" variant also displayed a significant higher hydrophobicity comparing with WT with a percentage of affinity to hexadecane of 34.3 ± 2.9% ($P < 0.05$). Variants exhibited growth rate in planktonic culture equal to 0.23 ± 0.06 h^{-1} for *mini*, 0.23 ± 0.05 h^{-1} for *rough*, and 0.22 ± 0.05 h^{-1} for *wrinkly*, which were not significantly different ($P > 0.05$) to that obtained for the WT (0.26 ± 0.04 h^{-1}) in M9 liquid medium supplemented with glucose (Table 1).

Genomic Characterization of *P. putida* KT2440 Variants

Whole genomes of WT and the three variants were sequenced using the Ion Torrent PGM® technology. Total number of reads reached 675,654 for *wrinkly*, 702,295 for *rough*, 944,384 for *mini*, and 1,075,826 for WT, respectively. The mean read length ranged from 233 to 259 bp that corresponding to a depth coverage of × 23.89, × 28.05, × 39.13, and × 40.16 for wrinkly, rough, mini, and WT strains, respectively. Mutations in variants identified after comparison with WT using CLC Genomics Workbench 6.0.1 are displayed in Table 2. Three mutations leading to a modification of amino acid sequences in coding regions were detected for the *mini* variant. The first was located in the *wbpM* gene (PP_1805) that encodes a polysaccharide biosynthesis protein and yields a stop codon at position 484 resulting in a truncated protein product. The second mutation was located in a region with a conserved domain coding for a major facilitator family transporter (PP_2830) homologous to the 4-hydroxyphenylacetate permease characterized in *Escherichia coli* (E-value = 4.44e-74). The third mutation in the *mini* variant was located in a gene coding a predicted carbamoyltransferase (PP_4944). The rough variant contained a threonine to proline substitution in a putative protein (PP_3030), upstream of a conserved sequence domain encoding a poly(R)-hydroxyalkanoic acid synthase subunit. The wrinkly variant contains a frameshift mutation at position 155 in the *lspA* gene (PP_0604) encoding a lipoprotein signal peptidase.

Table 1 Growth rates of *P. putida* KT2440 GFP (WT), variants, and their different combinations in planktonic suspensions. In combinations, overnight bacterial cultures were mixed to obtained equal numbers of cells for each strain in the growth medium at t_0

Strain combinations	Growth rates μ (h^{-1})
WT	0.26 ± 0.04
mini	0.23 ± 0.06
Wrinkly	0.23 ± 0.05
Rough	0.22 ± 0.05
WT + mini	0.31 ± 0.01
WT + rough	0.27 ± 0.02
WT + wrinkly	0.27 ± 0.01
WT + mini + rough	0.25 ± 0.05
WT + mini + wrinkly	0.30 ± 0.01
WT + rough + wrinkly	0.28 ± 0.01
WT + mini + rough + wrinkly	0.28 ± 0.02

Biofilm Architecture of *P. putida* KT2440 Variants

To assess the impact of identified mutations on biofilm architecture in variants, biofilms formed by the variants were then analyzed after 24 h and 168 h of development using CLSM and were compared with WT. After 24 h of development, the three variants produced biofilms with higher biovolumes than WT but after 168 h, only the *mini* variant significantly produced thicker biofilms (Fig. 3). Each variant exhibited specific biofilm architecture as showed in Fig. 3 by 3D reconstruction of biofilms and confocal slices at 168 h when compared with WT. The "mini" variant covered the entire surface available after 24 h of development and produced a dense and thick biofilm composed of numerous cell aggregates after 168 h of experiment. The "wrinkly" variant demonstrated the ability to form large and compact cell clusters under our experimental conditions. After 24 h of development, 3D clusters in the "wrinkly" variant biofilm were distinguished as shown in the illustrative 3D reconstruction in Fig. 3. At the end of the experiment, the "wrinkly" variant biofilm was composed of larger and denser aggregates than those observed for the WT. Although there is no striking difference between the "rough" variant and WT biofilms at 24 h of development, biofilm of the "rough" variant was mainly composed of intertwined chains of cells (such as those observed in liquid culture), and it did not form large cluster of cells after 168 h of development.

Competitive Advantages and Synergistic Association of Variants in Dual-Strain Biofilms

In order to assess the competitive advantage of the variants in biofilm, variants were first mixed each separately with the *P. putida* PCL1480 mCherry strain. After 24 h of development, the three variants demonstrated a better ability to survive in the presence of the *P. putida* PCL1480 mCherry strain in comparison with WT as illustrated by the ratio between GFP and mCherry biofilm biovolumes (Fig. 4). Interestingly, this was not the case after 24 h in a planktonic suspension as showed by the ratio obtained between KT2440 or variants and PCL1480 mCherry populations which were 1.86 ± 0.37, 1.11 ± 0.12, 1.63 ± 0.25, and 1.42 ± 0.52 for WT, mini, rough, and wrinkly, respectively. Such results demonstrated that variants did not exhibit an advantage versus PCL1480 mCherry strain in a planktonic culture compared with WT. After 168 h of development, only the "mini" variant exhibited a significant higher biovolume than mCherry strain PCL1480 and formed large 3D structures almost totally covering the PCL1480

Table 2 Mutations identified through Ion Torrent ® whole genome sequencing leading to protein modifications in variants in comparison with the *P. putida* KT2440 GFP strain (WT). Coverage (Cov.) refers to the number of times a single base is read during the sequencing. Frequency (Freq.) refers to the percentage of reads carrying the mutation

Strain	Locus	Annotation	Mutation	Cov.	Freq. (%)	Amino acid modification	Protein name
Mini	PP_1805	wbpM	C > A	52	98	Tyr 484 → stop	Polysaccharide biosynthesis protein
Mini	PP_2830		C > T	38	63	Arg 105 → Trp	Major facilitator family transporter
Mini	PP_4944		C > T	111	100	Gln 119 → stop	Carbamoyltransferase
Rough	PP_3030		A > C	29	45	Thr 93 → Pro	Hypothetical protein with conserved domain corresponding to Poly(R)-hydroxyalkanoic acid synthase subunit (PHA_synth_III_E)
Wrinkly	PP_0604	lspA	delG	29	52	Val155 → frameshift	Lipoprotein signal peptidase

mCherry strain. At 168 h of development in dual-strain biofilm, the "wrinkly" variant biofilm reaches a biovolume similar to that obtained for WT but clearly formed specific three-dimensional "mushroom-like" structures different to those produced by the WT. Only few cells of the "rough" variants persisted in the dual-strain biofilm at the end of the experiment, and mCherry PCL1480 biofilm had a lower biovolume than that obtained with WT showing a mutual inhibition between both strains.

In a second experiment, combinations of WT and one, two, or three variants were mixed together with the *P. putida* PCL1480 mCherry strain. Interestingly, we observed that the association of the three variants and WT produced thicker biofilms and has a better ability to compete with the mCherry PCL1480 strain than each variant separately as showed by 3D reconstructions and biovolumes values in Fig. 4 ($P < 0.05$).

As shown in Fig. 5, the ratios between the GFP and mCherry population biovolumes in the dual-strain biofilm were clearly higher in the case of the association of the 3 variants and WT, suggesting a synergistic effect of strain association in biofilm production and survival in the dual-strain biofilm with the PCL1480 mCherry strain. Overall, there was a correlation between the number of variants in the combinations and the value of the ratio between biovolumes of GFP and mCherry populations, that was especially noticeable after 24 h of development ($P < 0.05$) and to a lesser extent after 168 h. Moreover, we did not observe significant difference between growth rates in liquid suspension of WT alone or in combination with one, two, or three variants (Table 1) showing that potential strain interactions did not modify growth kinetic of the WT and derivatives in mixed population.

Discussion

To date, consequent numbers of works focused on the adaptation and the emergence of variants in microbial communities [15, 22, 23, 40–42] but few studies have begun to deal with the relation between pre-existing species and emergent

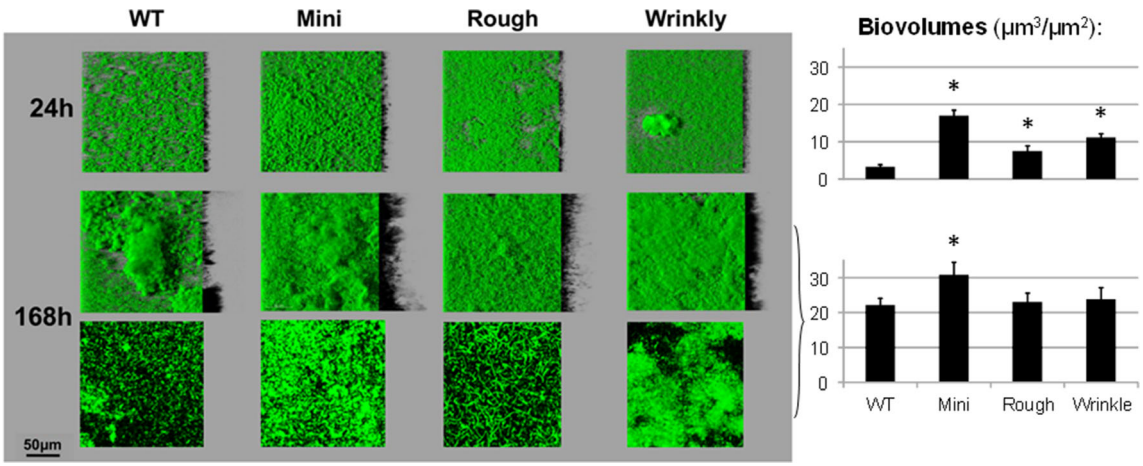

Fig. 3 Biofilm architecture and biovolumes of variants. Confocal slices were added to the 3D reconstruction for the 168-h time point. Error bars represent the standard deviation obtained with 10 confocal image stacks. Statistical significant difference observed with WT ($P < 0.05$) was indicated by an asterisk

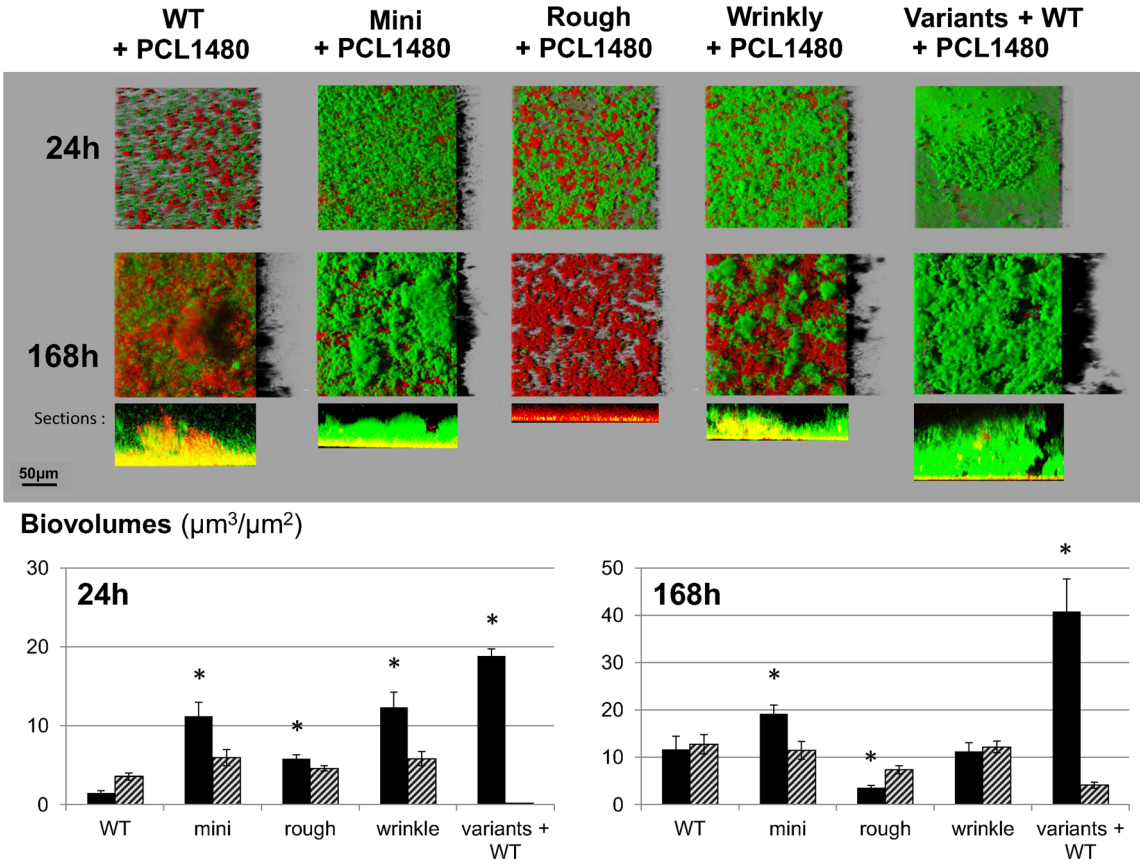

Fig. 4 Biofilm competition experiments between variants and *P. putida* PCL1480 mCherry. Images correspond to the aerial view of biofilms of mixed biofilms associating variants and the combination of variants and WT with the PCL1480 mCherry strain. Z-sections were also added for 168-h biofilms. In histograms, black bars correspond to the *P. putida* KT2440 GFP strain and dashed bars to the *P. putida* PCL1480 mCherry strain. Error bars represent the standard deviation obtained with 10 confocal image stacks. Statistical significant difference observed with WT ($P < 0.05$) was indicated by an asterisk

diversity (variants) in mixed microbial communities [30, 31]. In this study, we focused on the adaptation of the whole genome-sequenced strain *P. putida* KT2440 [43] alone or in response to intra-specific competition with another *P. putida* strain recently isolated from the environment (*P. putida* PCL1480 mCherry). *P. putida* KT2440 GFP was initially

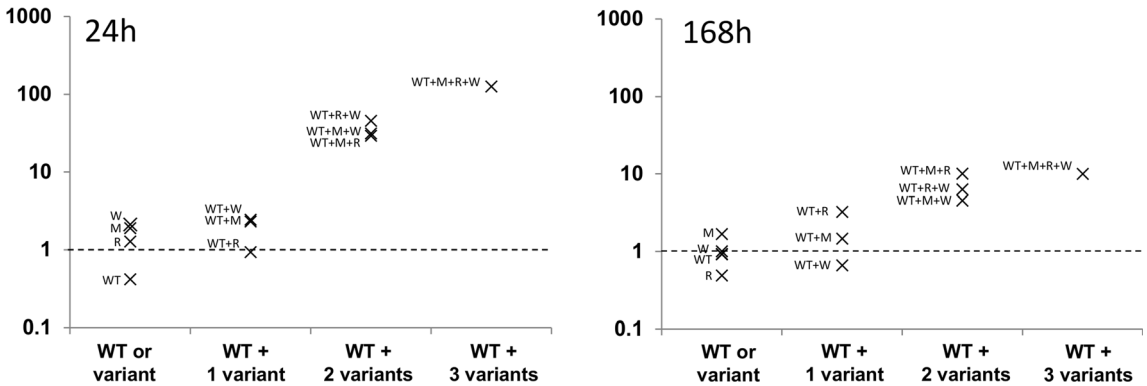

Fig. 5 Ratios between GFP (KT2440 and derivative) and PCL1480 mCherry population in mixed biofilms at 24 h and 168 h after development (variants were mixed in equal proportion, and GFP mixed population was inoculated at a ratio of 1:1 with the PCL 1480 strain). Data corresponding to the mean of the ratio between GFP and mCherry population biovolumes when (i) WT or one variant (each shown), (ii) WT paired with every variant, (iii) every combination of WT and 2 variants, or (iv) combination of WT and the three variants were mixed with the PCL1480 mCherry strain. For convenience, strain names were abbreviated on the figure: strain KT2440 WT, WT; Mini, M; Rough, R; and Wrinkly, W. Logarithmic scale was used for the *Y*-axis. Values superior to 1 (above the dotted line) illustrated that GFP population have a higher biovolume than mCherry population

outcompeted by the PCL1480 mCherry strain in the dual-strain biofilm at initial steps of the dynamic, but it was able to adapt to the PCL1480 mCherry strain and produced biofilm with similar biovolume after 168 h of co-culture (Fig. 1), that coincide with the emergence of KT2440 genetic variants with specific phenotypes. The production and selection of genetic variants indeed constitute one of the described mechanisms of adaptation in various species [19–26], and some evidences suggest that biofilm could favor the emergence of a genetic diversity by providing specific micro-environmental conditions to bacteria [18, 44, 45]. Such observations are here supported by the fact that we did not detect any variants after a planktonic co-culture of 168 h associating *P. putida* KT2440 GFP and the mCherry strain. In addition, since we did not observe the emergence of colony morphology variants in the KT2440 GFP axenic cultures, it is tempting to speculate that the selection pressures are more important in the mixed culture and thus that species or even strain diversity may favor the emergence of genetic diversity in microbial communities. In agreement with this, Lawrence et al. [30] found that species from the roots of a beech tree evolved more in diverse species mixtures than it did when cultured in isolation. However, other findings revealed that the percentage of morphotypic variants tended to decrease with the increasing interspecific community diversity in mixed biofilms with *Pseudomonas fluorescens*, *K. pneumonia*, and *P. aeruginosa* [46]. Therefore, the impact of species diversity on genetic diversification in biofilm might highly depend on the strains involved and on the nature of their interactions.

Here, three morphological colony variants called *mini*, *rough*, and *wrinkly* were produced in the mixed biofilm. Despite numerous subcultures on TSA plate, their morphotypes were stable illustrating heritable characteristics as opposed to transient gene expression [47]. These variants exhibited specific phenotypes in terms of cellular morphology, cell surface properties, swimming or swarming abilities, and biofilm architecture (Figs. 2 and 3) and displayed overall a better ability to survive with the PCL1480 mCherry strain compared with WT in dual-strain biofilms (Fig. 4). Interestingly, specific phenotypes of the variants did not improve their fitness in the presence of the mCherry strain in a planktonic co-culture showing these adaptations, and their better ability to survive with the PCL1480 mCherry strain are not a general feature but rather a specific adaptation to the dual-biofilm conditions. Sequencing of the whole genomes of these variants and their comparison with WT (KT2440 GFP) enables the identification of mutations involved (Table 2). A mutation in the *wbpM* gene which encodes a highly conserved protein involved in the biosynthesis of polysaccharides was found in *mini* variant. WbpM have been described as an inner membrane UDP-GlcNAc C6 dehydratase essential in the biosynthesis of B-band of lipopolysaccharides (LPS) in *P. aeruginosa*, and *wbpM* homologs that are required for LPS or capsule biosynthesis have also been found in numerous bacteria including Gram-positive bacteria [48, 49]. Modification of such membrane-associated element has been already shown to directly impact the cell surface properties and thus cell-cell and cell surface interactions resulting in a modification of biofilm architecture in different species including *P. putida* [41, 50, 51]. Interestingly, Penterman et al. [41] reported in *P. aeruginosa* that mutations in gene involved in B-band LPS acquired after the adaptation of cells to the biofilm way of life provided a strong biofilm fitness advantage, increasing from 1 to over 50% of the biofilm population after only 3 days. The observed increasing biovolume and specific architecture of variant *mini* biofilm could be partly related to the very high hydrophobicity of cells resulting from the modification of LPS that increased the cohesiveness in the biofilm and thus enhanced the formation of dense biofilm aggregates as already proposed for *Streptococcus pneumonia, Pseudomonas aeruginosa*, or *Bradyrhizobium japonicum* for instance [20, 52, 53]. Such features of the *mini* variant could thus explain its ability to produce more biofilm than WT and could also play a role in the competition with the *P. putida* PCL1480 mCherry strain. The second mutation found in the *mini* variant was located in a major facilitator transporter with a conserved domain corresponding to the 4-hydroxyphenylacetate (4-HPA) permease, a transport system for 4-HPA initially identified in *Escherichia coli* [54]. Although the link between the 4-HPA transport and the biofilm phenotype of the *mini* variant is not direct, the mutation in the membrane transporter could alter bacterial cell surface properties and thus modify interaction of bacteria with each other and with the surface leading to a modification of biofilm three-dimensional structure. This is reminiscent of previous studies reporting that mutations in membrane transporter can indeed lead to a modification of biofilm architecture in mutants [55, 56]. The third mutation in the mini variant was found in a gene coding a predicted carbamoyltransferase which is an enzyme participating to the post-translational modification of proteins by adding carbamoyl functional group. Such enzyme could be involved in number of central metabolic reactions in *P. putida* such as pyrimidine nucleotides synthesis or citrulline metabolism [57–59] and its modification could thus also impact biofilm formation throughout central metabolic pathways.

The wrinkly variant is mutated in the *lspA* gene coding a lipoprotein signal peptidase that likely lead to a modification of both the structure and the bacterial localization of the lipoproteins produced. Phenotypically, we observed that such mutation leads to a modification of cell morphology and cell hydrophobicity, to the ability to swarm and to form pellicle at the air-medium interface. This mutation also modified biofilm architecture in *wrinkly* variant and its fitness with the PCL1480 mCherry strain in dual-strain biofilm. In agreement with these results, an analysis of random transposon

hyperadherent mutants in the same strain *P. putida* KT2440 showed that a mutation in a gene coding an outer membrane lipoprotein led to (i) an increased adhesion in the early early time of biofilm development, (ii) the modification of biofilm architecture, and (iii) the partial restoration of swarming ability compared with WT [60]. This suggests an important role of lipoproteins in *P. putida* multicellular development as described in other species [61–63].

Intriguingly, we observed that the *rough* variant was able to better outcompete the PCL1480 mCherry strain after 24 h of development compared with WT but not after 168 h. Indeed, a mutual inhibition between both strains occurred in the end of structural dynamic as revealed by biofilm biovolume values (Figs. 3 and 4). Genomic analyses revealed that rough variant carries a mutation upstream a conserved domain corresponding to the Poly(R)-hydroxyalkanoic acid (PHA) synthase subunit, PhaE. In *P. putida*, PHA synthesis directly competes with the production of the rhamnolipid precursor [64, 65]. It is thus possible that, in our case, an alteration of the *phaE* expression leads to a modification of rhamnolipid yield in *rough* variant. Rhamnolipids are the most important classes of bacterial surfactants and are known to play multiple roles in bacteria as they enhance the uptake of hydrophobic substrates, display potential antimicrobials activities, are virulence factors, promote surface motility, and affect biofilm development and architecture [66–68]. Indeed, it has been shown that dispersal of settled biofilm is partly dependent on rhamnolipids in *P. aeruginosa* [69]. Rhamnolipids can also be used as a defense mechanism by preventing outside bacteria from colonizing the available remaining surface and thus avoiding detrimental effect for the established community [69–72]. From these observations, the potential modification of rhamnolipid production in rough variant could explain its better ability to compete with the PCL1480 mCherry strain after 24 h of development and also the fact that we observed a lower number of cells after 168 h for both the rough variant and the PCL1480 mCherry strain in the flow cell due to the dispersal effect of rhamnolipids. When looking the strategy of the rough variant independently, we can thus conclude that this variation was not really beneficial. However, in the light of the biovolumes ratio obtained between GFP and mCherry population in mixed communities when the *rough* variant was associated with WT and one or both other variants, we observed that the whole GFP population benefits from the presence of the *rough* variant showing a better ability to compete with the PCL1480 mCherry strain (Figs. 4 and 5). The fact that this phenomenon was more noticeable at 24 h and to a lesser degree at 168 h may be partly explained by the adaptation of the mCherry population during the course of the dual-strain biofilm development. These observations suggested strong interactions between rough and other GFP strains and potentially an altruistic behavior of the *rough* variant. We observed in the present work that the association of the three variants and WT constitutes the population with the highest fitness with respect to the ratio obtained between GFP and mCherry populations in mixed communities (Fig. 5). Indeed, such strain association demonstrated the ability to outcompete the PCL1480 strain by producing population with a biovolume approximately two times higher than those obtained for the *mini* variant, which was the better biofilm producer (Fig. 4). As the total number of cells introduced in the flow cell at the beginning of each experiment is the same, the difference observed in terms of biofilm production is likely due to specific synergistic interactions between the different variants. The fact that variant and WT association did not lead to an increase of growth rate of the whole GFP (WT and variants) population in liquid culture (Table 1) suggested that such characteristics of the WT and variant association was not due to a growth rate increase of one or more GFP variants in the mix but rather arose from the concomitant expression and the interaction of the specific features of variant involved in biofilm formation and competition. Globally, these results demonstrated that the mutations undergone by *P. putida* KT2440 result in the emergence of variant strains with specific and complementary survival strategies that lead to a synergistic adaptation of the KT2440 population in the dual-strain biofilm. Similar results were reported on *Burkholderia cenocepacia* through the analysis of the mutational patterns of a single biofilm community during long-term experiments [23, 26]. The authors demonstrated that when variants are grown together, mixed community is more productive than any one type grown alone suggesting a synergistic effect of all ecotypes association. Interestingly, by studying the evolution of a mixed community composed of five species, Lawrence et al. [30] demonstrated that each species evolved divergently to use waste products generated by other species, leading to the emergence of a complementary cross-feeding strategy at the scale of the whole population. The resulting mixed community of co-evolved bacteria used more of the available resources and thus displayed an enhanced productivity compared with the same group of species that evolved in isolation.

In this study, the nature of the specific WT and variant interactions remained unclear but it could be related to modified cell-cell and cell surface adhesion properties between variant strains due to the modification of different extracellular components such as lipoprotein in *wrinkly* variant or LPS in *mini* variant that increase their cell surface hydrophobicity. The role of the potential modification of rhamnolipids production in rough variant could also play a role in the specific interactions between WT and variant strains of KT2440. Further dedicated studies are required to better identify the specific molecular pathways involved in such synergistic interactions.

In conclusion, this work provides evidence that an intraspecific competition can foster the emergence of various phenotypes that increases together the global fitness of the

resulting population. The community thus evolved through the generation of new genetic variation (diversification) and a selection based on collective fitness advantages of new variants [73]. It underlined the importance of interactions in the evolution and adaptation of microbial species and the fact that data obtained from single-species models are not directly transposable to environmental communities given that the vast majority of species interact with each other in nature. Moreover, this work highlighted the importance of synergic interactions within the emergent diversity in this adaptation process.

Acknowledgments Claus Sternberg is acknowledged for the kind gift of the *P. putida* KT2440 GFP strain and Ellen Lagendijk for the *P.putida* PCL1480 mCherry strain.

Funding Information This work was funded by the French National Research Agency (ANR) within the SYSCOMM project DISCO (ANR-09-SYSC-003). This study was conducted on the LABE experimental platform funded by DRRT in the framework of CPER 2007–2013 projects.

References

1. Flemming HC, Wuertz S (2019) Bacteria and archaea on earth and their abundance in biofilms. Nat Rev Microbiol 17:247–260. https://doi.org/10.1038/s41579-019-0158-9
2. Hojo K, Nagaoka S, Ohshima T, Maeda N (2009) Bacterial interactions in dental biofilm development. J Dent Res 88:982–990. https://doi.org/10.1177/0022034509346811
3. Li YH, Tian X (2012) Quorum sensing and bacterial social interactions in biofilms. Sensors 12:2519–2538. https://doi.org/10.3390/s120302519
4. Bridier A, Briandet R, Bouchez T, Jabot F (2014) A model-based approach to detect interspecific interactions during biofilm development. Biofouling 30:761–771. https://doi.org/10.1080/08927014.2014.923409
5. Lykidis A, Chen CL, Tringe SG, McHardy AC, Copeland A, Kyrpides NC, Hugenholtz P, Macarie H, Olmos A, Monroy O, Liu WT (2011) Multiple syntrophic interactions in a terephthalate-degrading methanogenic consortium. ISME J 5:122–130. https://doi.org/10.1038/ismej.2010.125
6. Sieber JR, McInerney MJ, Gunsalus RP (2012) Genomic insights into syntrophy: the paradigm for anaerobic metabolic cooperation. Annu Rev Microbiol 66:429–452. https://doi.org/10.1146/annurev-micro-090110-102844
7. Kato S, Watanabe K (2010) Ecological and evolutionary interactions in syntrophic methanogenic consortia. Microbes Environ 25:145–151
8. Ren D, Madsen JS, Sorensen SJ, Burmolle M (2014) High prevalence of biofilm synergy among bacterial soil isolates in cocultures indicates bacterial interspecific cooperation. ISME J. https://doi.org/10.1038/ismej.2014.96
9. Bridier A, Sanchez-Vizuete Mdel P, Le Coq D, Aymerich S, Meylheuc T, Maillard JY, Thomas V, Dubois-Brissonnet F, Briandet R (2012) Biofilms of a Bacillus subtilis hospital isolate protect Staphylococcus aureus from biocide action. PLoS One 7:e44506. https://doi.org/10.1371/journal.pone.0044506
10. Lee KW, Periasamy S, Mukherjee M, Xie C, Kjelleberg S, Rice SA (2014) Biofilm development and enhanced stress resistance of a model, mixed-species community biofilm. ISME J 8:894–907. https://doi.org/10.1038/ismej.2013.194
11. Sanchez-Vizuete P, Le Coq D, Bridier A, Herry JM, Aymerich S, Briandet R (2015) Identification of ypqP as a new Bacillus subtilis biofilm determinant that mediates the protection of Staphylococcus aureus against antimicrobial agents in mixed-species communities. Appl Environ Microbiol 81:109–118. https://doi.org/10.1128/AEM.02473-14
12. Burmolle M, Ren D, Bjarnsholt T, Sorensen SJ (2014) Interactions in multispecies biofilms: do they actually matter? Trends Microbiol 22:84–91. https://doi.org/10.1016/j.tim.2013.12.004
13. Zhang QG, Buckling A, Ellis RJ, Godfray HC (2009) Coevolution between cooperators and cheats in a microbial system. Evolution 63:2248–2256. https://doi.org/10.1111/j.1558-5646.2009.00708.x
14. Bridier A, Piard JC, Pandin C, Labarthe S, Dubois-Brissonnet F, Briandet R (2017) Spatial organization plasticity as an adaptive driver of surface microbial communities. Front Microbiol 8:1364. https://doi.org/10.3389/fmicb.2017.01364
15. McElroy KE, Hui JG, Woo JK, Luk AW, Webb JS, Kjelleberg S, Rice SA, Thomas T (2014) Strain-specific parallel evolution drives short-term diversification during Pseudomonas aeruginosa biofilm formation. Proc Natl Acad Sci U S A 111:E1419–E1427. https://doi.org/10.1073/pnas.1314340111
16. Boles BR, Thoendel M, Singh PK (2004) Self-generated diversity produces "insurance effects" in biofilm communities. Proc Natl Acad Sci U S A 101:16630–16635. https://doi.org/10.1073/pnas.0407460101
17. Steenackers HP, Parijs I, Dubey A, Foster KR, Vanderleyden J (2016) Experimental evolution in biofilm populations. FEMS Microbiol Rev 40:373–397. https://doi.org/10.1093/femsre/fuw002
18. Martin M, Holscher T, Dragos A, Cooper VS, Kovacs AT (2016) Laboratory evolution of microbial interactions in bacterial biofilms. J Bacteriol 198:2564–2571. https://doi.org/10.1128/JB.01018-15
19. Lujan AM, Macia MD, Yang L, Molin S, Oliver A, Smania AM (2011) Evolution and adaptation in Pseudomonas aeruginosa biofilms driven by mismatch repair system-deficient mutators. PLoS One 6:e27842. https://doi.org/10.1371/journal.pone.0027842
20. Allegrucci M, Sauer K (2007) Characterization of colony morphology variants isolated from Streptococcus pneumoniae biofilms. J Bacteriol 189:2030–2038. https://doi.org/10.1128/JB.01369-06
21. Yildiz FH, Schoolnik GK (1999) Vibrio cholerae O1 El Tor: identification of a gene cluster required for the rugose colony type, exopolysaccharide production, chlorine resistance, and biofilm formation. Proc Natl Acad Sci U S A 96:4028–4033
22. Workentine ML, Harrison JJ, Weljie AM, Tran VA, Stenroos PU, Tremaroli V, Vogel HJ, Ceri H, Turner RJ (2010) Phenotypic and metabolic profiling of colony morphology variants evolved from Pseudomonas fluorescens biofilms. Environ Microbiol 12:1565–1577. https://doi.org/10.1111/j.1462-2920.2010.02185.x
23. Poltak SR, Cooper VS (2011) Ecological succession in long-term experimentally evolved biofilms produces synergistic communities. ISME J 5:369–378. https://doi.org/10.1038/ismej.2010.136
24. Ponciano JM, La HJ, Joyce P, Forney LJ (2009) Evolution of diversity in spatially structured Escherichia coli populations. Appl Environ Microbiol 75:6047–6054. https://doi.org/10.1128/AEM.00063-09
25. Yarwood JM, Paquette KM, Tikh IB, Volper EM, Greenberg EP (2007) Generation of virulence factor variants in Staphylococcus aureus biofilms. J Bacteriol 189:7961–7967. https://doi.org/10.1128/JB.00789-07
26. Traverse CC, Mayo-Smith LM, Poltak SR, Cooper VS (2013) Tangled bank of experimentally evolved Burkholderia biofilms reflects selection during chronic infections. Proc Natl Acad Sci U S A 110:E250–E259. https://doi.org/10.1073/pnas.1207025110
27. Starkey M, Hickman JH, Ma L, Zhang N, De Long S, Hinz A, Palacios S, Manoil C, Kirisits MJ, Starner TD, Wozniak DJ,

Harwood CS, Parsek MR (2009) Pseudomonas aeruginosa rugose small-colony variants have adaptations that likely promote persistence in the cystic fibrosis lung. J Bacteriol 191:3492–3503. https://doi.org/10.1128/JB.00119-09
28. Beyhan S, Bilecen K, Salama SR, Casper-Lindley C, Yildiz FH (2007) Regulation of rugosity and biofilm formation in Vibrio cholerae: comparison of VpsT and VpsR regulons and epistasis analysis of vpsT, vpsR, and hapR. J Bacteriol 189:388–402. https://doi.org/10.1128/JB.00981-06
29. Li W, Li Y, Wu Y, Cui Y, Liu Y, Shi X, Zhang Q, Chen Q, Sun Q, Hu Q (2016) Phenotypic and genetic changes in the life cycle of small colony variants of Salmonella enterica serotype Typhimurium induced by streptomycin. Ann Clin Microbiol Antimicrob 15:37–11. https://doi.org/10.1186/s12941-016-0151-3
30. Lawrence D, Fiegna F, Behrends V, Bundy JG, Phillimore AB, Bell T, Barraclough TG (2012) Species interactions alter evolutionary responses to a novel environment. PLoS Biol 10:e1001330. https://doi.org/10.1371/journal.pbio.1001330
31. Hansen SK, Rainey PB, Haagensen JA, Molin S (2007) Evolution of species interactions in a biofilm community. Nature 445:533–536. https://doi.org/10.1038/nature05514
32. Freilich S, Zarecki R, Eilam O, Segal ES, Henry CS, Kupiec M, Gophna U, Sharan R, Ruppin E (2011) Competitive and cooperative metabolic interactions in bacterial communities. Nat Commun 2:589. https://doi.org/10.1038/Ncomms1597
33. Kuiper I, Lagendijk EL, Pickford R, Derrick JP, Lamers GE, Thomas-Oates JE, Lugtenberg BJ, Bloemberg GV (2004) Characterization of two Pseudomonas putida lipopeptide biosurfactants, putisolvin I and II, which inhibit biofilm formation and break down existing biofilms. Mol Microbiol 51:97–113
34. Lambertsen L, Sternberg C, Molin S (2004) Mini-Tn7 transposons for site-specific tagging of bacteria with fluorescent proteins. Environ Microbiol 6:726–732. https://doi.org/10.1111/j.1462-2920.2004.00605.x
35. Lagendijk EL, Validov S, Lamers GEM, de Weert S, Bloemberg GV (2010) Genetic tools for tagging Gram-negative bacteria with mCherry for visualization in vitro and in natural habitats, biofilm and pathogenicity studies. FEMS Microbiol Lett 305:81–90. https://doi.org/10.1111/j.1574-6968.2010.01916.x
36. Weiss Nielsen M, Sternberg C, Molin S, Regenberg B (2011) Pseudomonas aeruginosa and Saccharomyces cerevisiae biofilm in flow cells. J Vis Exp 47:e2383. https://doi.org/10.3791/2383
37. Heydorn A, Nielsen AT, Hentzer M, Sternberg C, Givskov M, Ersboll BK, Molin S (2000) Quantification of biofilm structures by the novel computer program COMSTAT. Microbiol-Uk 146: 2395–2407
38. Rosenberg M, Gutnick D, Rosenberg E (1980) Adherence of bacteria to hydrocarbons-a simple method for measuring cell-surface hydrophobicity. FEMS Microbiol Lett 9:29–33
39. Cheroutre-Vialette M, Lebert I, Hebraud M, Labadie JC, Lebert A (1998) Effects of pH or a(w) stress on growth of Listeria monocytogenes. Int J Food Microbiol 42: 71-77.
40. Lenski RE, Travisano M (1994) Dynamics of adaptation and diversification: a 10,000-generation experiment with bacterial populations. Proc Natl Acad Sci U S A 91:6808–6814
41. Penterman J, Nguyen D, Anderson E, Staudinger BJ, Greenberg EP, Lam JS, Singh PK (2014) Rapid evolution of culture-impaired bacteria during adaptation to biofilm growth. Cell Rep 6:293–300. https://doi.org/10.1016/j.celrep.2013.12.019
42. Flynn KM, Dowell G, Johnson TM, Koestler BJ, Waters CM, Cooper VS (2016) Evolution of ecological diversity in biofilms of Pseudomonas aeruginosa by altered cyclic diguanylate signaling. J Bacteriol 198:2608–2618. https://doi.org/10.1128/JB.00048-16
43. Nelson KE, Weinel C, Paulsen IT, Dodson RJ, Hilbert H, Martins dos Santos VA, Fouts DE, Gill SR, Pop M, Holmes M, Brinkac L, Beanan M, DeBoy RT, Daugherty S, Kolonay J, Madupu R, Nelson W, White O, Peterson J, Khouri H, Hance I, Chris Lee P, Holtzapple E, Scanlan D, Tran K, Moazzez A, Utterback T, Rizzo M, Lee K, Kosack D, Moestl D, Wedler H, Lauber J, Stjepandic D, Hoheisel J, Straetz M, Heim S, Kiewitz C, Eisen JA, Timmis KN, Dusterhoft A, Tummler B, Fraser CM (2002) Complete genome sequence and comparative analysis of the metabolically versatile Pseudomonas putida KT2440. Environ Microbiol 4:799–808
44. Conibear TC, Collins SL, Webb JS (2009) Role of mutation in Pseudomonas aeruginosa biofilm development. PLoS One 4: e6289. https://doi.org/10.1371/journal.pone.0006289
45. Driffield K, Miller K, Bostock JM, O'Neill AJ, Chopra I (2008) Increased mutability of Pseudomonas aeruginosa in biofilms. J Antimicrob Chemother 61:1053–1056. https://doi.org/10.1093/jac/dkn044
46. Kelvin Lee KW, Hoong Yam JK, Mukherjee M, Periasamy S, Steinberg PD, Kjelleberg S, Rice SA (2016) Interspecific diversity reduces and functionally substitutes for intraspecific variation in biofilm communities. ISME J 10:846–857. https://doi.org/10.1038/ismej.2015.159
47. Koh KS, Lam KW, Alhede M, Queck SY, Labbate M, Kjelleberg S, Rice SA (2007) Phenotypic diversification and adaptation of Serratia marcescens MG1 biofilm-derived morphotypes. J Bacteriol 189:119–130. https://doi.org/10.1128/Jb.00930-06
48. Burrows LL, Urbanic RV, Lam JS (2000) Functional conservation of the polysaccharide biosynthetic protein WbpM and its homologues in Pseudomonas aeruginosa and other medically significant bacteria. Infect Immun 68:931–936. https://doi.org/10.1128/Iai.68.2.931-936.2000
49. Creuzenet C, Lam JS (2001) Topological and functional characterization of WbpM, an inner membrane UDP-GlcNAc C6 dehydratase essential for lipopolysaccharide biosynthesis in Pseudomonas aeruginosa. Mol Microbiol 41:1295–1310
50. Hansen SK, Haagensen JAJ, Gjermansen M, Jorgensen TM, Tolker-Nielsen T, Molin S (2007) Characterization of a Pseudomonas putida rough variant evolved in a mixed-species biofilm with Acinetobacter sp strain C6. J Bacteriol 189:4932–4943. https://doi.org/10.1128/Jb.00041-07
51. Lau PCY, Lindhout T, Beveridge TJ, Dutcher JR, Lam JS (2009) Differential lipopolysaccharide core capping leads to quantitative and correlated modifications of mechanical and structural properties in Pseudomonas aeruginosa biofilms. J Bacteriol 191:6618–6631. https://doi.org/10.1128/Jb.00698-09
52. Kirisits MJ, Prost L, Starkey M, Parsek MR (2005) Characterization of colony morphology variants isolated from Pseudomonas aeruginosa biofilms. Appl Environ Microbiol 71: 4809–4821. https://doi.org/10.1128/AEM.71.8.4809-4821.2005
53. Lee YW, Jeong SY, In YH, Kim KY, So JS, Chang WS (2010) Lack of O-polysaccharide enhances biofilm formation by Bradyrhizobium japonicum. Lett Appl Microbiol 50:452–456. https://doi.org/10.1111/j.1472-765X.2010.02813.x
54. Prieto MA, Garcia JL (1997) Identification of the 4-hydroxyphenylacetate transport gene of Escherichia coli W: construction of a highly sensitive cellular biosensor. FEBS Lett 414: 293–297
55. Zhu X, Long F, Chen Y, Knochel S, She Q, Shi X (2008) A putative ABC transporter is involved in negative regulation of biofilm formation by Listeria monocytogenes. Appl Environ Microbiol 74: 7675–7683. https://doi.org/10.1128/AEM.01229-08
56. Hinsa SM, Espinosa-Urgel M, Ramos JL, O'Toole GA (2003) Transition from reversible to irreversible attachment during biofilm formation by Pseudomonas fluorescens WCS365 requires an ABC transporter and a large secreted protein. Mol Microbiol 49:905–918
57. Wargnies B, Legrain C, Stalon V (1978) Anabolic ornithine carbamoyltransferase of Escherichia coli and catabolic ornithine carbamoyltransferase of Pseudomonas putida. Steady-state kinetic analysis. Eur J Biochem 89:203–212

58. Falmagne P, Portetelle D, Stalon V (1985) Immunological and structural relatedness of catabolic ornithine carbamoyltransferases and the anabolic enzymes of enterobacteria. J Bacteriol 161:714–719
59. Schurr MJ, Vickrey JF, Kumar AP, Campbell AL, Cunin R, Benjamin RC, Shanley MS, O'Donovan GA (1995) Aspartate transcarbamoylase genes of Pseudomonas putida: requirement for an inactive dihydroorotase for assembly into the dodecameric holoenzyme. J Bacteriol 177:1751–1759
60. Yousef-Coronado F, Soriano MI, Yang L, Molin S, Espinosa-Urgel M (2011) Selection of hyperadherent mutants in Pseudomonas putida biofilms. Microbiology 157: 2257-2265. https://doi.org/10.1099/mic.0.047787-0
61. Vasseur P, Soscia C, Voulhoux R, Filloux A (2007) PelC is a Pseudomonas aeruginosa outer membrane lipoprotein of the OMA family of proteins involved in exopolysaccharide transport. Biochimie 89:903–915. https://doi.org/10.1016/j.niochi.2007.04.002
62. Uhlich GA, Gunther NW, Bayles DO, Mosier DA (2009) The CsgA and Lpp proteins of an Escherichia coli O157:H7 strain affect HEp-2 cell invasion, motility, and biofilm formation. Infect Immun 77:1543–1552. https://doi.org/10.1128/Iai.00949-08
63. Connelly MB, Young GA, Sloma A (2004) Extracellular proteolytic activity plays a central role in swarming motility in Bacillus subtilis. J Bacteriol 186:4159–4167. https://doi.org/10.1128/Jb.186.13.4159-4167.2004
64. Choi MH, Xu J, Gutierrez M, Yoo T, Cho YH, Yoon SC (2011) Metabolic relationship between polyhydroxyalkanoic acid and rhamnolipid synthesis in Pseudomonas aeruginosa: comparative (1)(3)C NMR analysis of the products in wild-type and mutants. J Biotechnol 151:30–42. https://doi.org/10.1016/j.jbiotec.2010.10.072
65. Wittgens A, Tiso T, Arndt TT, Wenk P, Hemmerich J, Muller C, Wichmann R, Kupper B, Zwick M, Wilhelm S, Hausmann R, Syldatk C, Rosenau F, Blank LM (2011) Growth independent rhamnolipid production from glucose using the non-pathogenic Pseudomonas putida KT2440. Microb Cell Factories 10:80. https://doi.org/10.1186/1475-2859-10-80
66. Gutierrez M, Choi MH, Tian B, Xu J, Rho JK, Kim MO, Cho YH, Yoon SC (2013) Simultaneous inhibition of rhamnolipid and polyhydroxyalkanoic acid synthesis and biofilm formation in Pseudomonas aeruginosa by 2-bromoalkanoic acids: effect of inhibitor alkyl-chain-length. PloS One 8:e73986. https://doi.org/10.1371/journal.pone.0073986
67. Abdel-Mawgoud AM, Lepine F, Deziel E (2010) Rhamnolipids: diversity of structures, microbial origins and roles. Appl Microbiol Biotechnol 86:1323–1336. https://doi.org/10.1007/s00253-010-2498-2
68. Davey ME, Caiazza NC, O'Toole GA (2003) Rhamnolipid surfactant production affects biofilm architecture in Pseudomonas aeruginosa PAO1. J Bacteriol 185:1027–1036. https://doi.org/10.1128/Jb.185.3.1027-1036.2003
69. Boles BR, Thoendel M, Singh PK (2005) Rhamnolipids mediate detachment of Pseudomonas aeruginosa from biofilms. Mol Microbiol 57:1210–1223. https://doi.org/10.1111/j.1365-2958.2005.04743.x
70. Dusane DH, Nancharaiah YV, Zinjarde SS, Venugopalan VP (2010) Rhamnolipid mediated disruption of marine Bacillus pumilus biofilms. Colloid Surf B 81:242–248. https://doi.org/10.1016/j.colsurfb.2010.07.013
71. Irie Y, O'Toole GA, Yuk MH (2005) Pseudomonas aeruginosa rhamnolipids disperse Bordetella bronchiseptica biofilms. FEMS Microbiol Lett 250:237–243. https://doi.org/10.1016/j.femsle.2005.07.012
72. Espinosa-Urgel M (2003) Resident parking only: rhamnolipids maintain fluid channels in biofilms. J Bacteriol 185:699–700. https://doi.org/10.1128/Jb.185.3.699-700.2003
73. Nemergut DR, Schmidt SK, Fukami T, O'Neill SP, Bilinski TM, Stanish LF, Knelman JE, Darcy JL, Lynch RC, Wickey P, Ferrenberg S (2013) Patterns and processes of microbial community assembly. Microbiol Mol Biol Rev 77:342–356. https://doi.org/10.1128/MMBR.00051-12